

# Color space transformations for digital photography exploiting information about the illuminant estimation process

Simone Bianco,<sup>1,\*</sup> Arcangelo Bruna,<sup>2</sup> Filippo Naccari,<sup>2</sup> and Raimondo Schettini<sup>1</sup>

<sup>1</sup>*DISCo—Dipartimento di Informatica, Sistemistica e Comunicazione, Università degli Studi di Milano-Bicocca, Viale Sarca 336, 20126 Milano, Italy*

<sup>2</sup>*STMicronics—Advanced System Technology—Catania Lab, Catania, Italy*

*\*Corresponding author: simone.bianco@disco.unimib.it*

Received August 16, 2011; revised October 19, 2011; accepted December 1, 2011; posted December 2, 2011 (Doc. ID 153006); published February 28, 2012

The color reproduction accuracy is a key factor to the overall perceived image quality in digital photography. In this framework, both the illuminant estimation process and the color correction matrix concur in the formation of the overall perceived image quality. To the best of our knowledge, the two processes have always been studied separately, thus ignoring the interactions between them. We investigate here these interactions, showing how the color correction transform amplifies the illuminant estimation errors. We demonstrate that incorporating knowledge about the illuminant estimation behavior in the optimization of the color correction matrix makes it possible to alleviate the error amplification. Different strategies to improve color accuracy under both perfect and imperfect white point estimations are investigated, and the experimental results obtained with a digital camera simulator are reported. © 2012 Optical Society of America

OCIS codes: 100.0100, 330.1710.

## 1. INTRODUCTION

The color reproduction accuracy of digital imaging acquisition devices is a key factor to the overall perceived image quality [1]. The first stage of the color correction pipeline [1] aims to estimate and compensate for the color of the illuminant in the scene, rendering the acquired objects as if they were lit by an ideal illuminant [2]. The second stage of the color correction pipeline is the device chromatic response characterization that transforms the image data into a standard RGB color space. This transformation, usually called color matrixing, is needed because the spectral sensitivity functions of the sensor color channels rarely match those of the desired output color space. This transformation is usually performed using a linear transformation matrix, and it is optimized assuming that the illuminant in the scene has been successfully estimated and compensated for [3,4]. Both the illuminant estimation process and the color correction matrix concur in the formation of the overall perceived image quality. To the best of our knowledge, the two processes have always been studied separately, thus ignoring the interactions between them.

In this paper we investigate the interactions between the illuminant estimation process and the color correction matrix in the formation of the overall color accuracy, especially when the white point estimation is imperfect. We also investigate how the color correction transform amplifies the illuminant estimation errors. The only work we found on a related topic [5] analyzes the error propagation in color measurement and imaging focusing on how linear, matrix, and nonlinear

transformations influence the mean, variance, and covariance of color measurements. The error analyzed by Burns and Berns [5] is the measurement noise, while, in this paper, we analyze the error introduced by the modules of the imaging pipeline. In Section 2, we briefly describe the image formation process and a simplified color correction pipeline. In Sections 3 and 4, it is shown how to derive illuminant varying color correction matrices and how to incorporate information about the illuminant estimation process in the derivation of the color correction matrix to alleviate the error amplification. The experimental results are derived under both ideal and nonideal illuminant estimation conditions and are described in Sections 5 and 6. Finally, in Section 7, conclusions are drawn.

## 2. COLOR CORRECTION PIPELINE

An image acquired by a digital camera can be represented as a function  $\rho$  mainly dependent on three physical factors: the illuminant spectral power distribution  $I(\lambda)$ , the surface spectral reflectance  $S(\lambda)$  and the sensor spectral sensitivities  $C(\lambda)$ . Using this notation, the sensor responses at the pixel with coordinates  $(x, y)$  can be thus described as

$$\rho(x, y) = \int_{\omega} I(\lambda)S(x, y, \lambda)C(\lambda)d\lambda, \quad (1)$$

where  $\omega$  is the wavelength range of the visible light spectrum,  $\rho$  and  $C(\lambda)$  are three-component vectors. Since the three sensor spectral sensitivities are usually, respectively, more

sensitive to the low, medium, and high wavelengths, the three-component vector of sensor responses  $\rho = (\rho_1, \rho_2, \rho_3)$  is also referred to as the sensor or camera raw **RGB** =  $(R, G, B)$  triplet. Usually the image sensor is composed of three different photo-receptors acquiring red, green and blue color components, displaced following the Bayer pattern [6]. In the following, we adopt the convention that **RGB** triplets are represented by column vectors.

The first stage of the color correction pipeline aims to estimate and compensate for the color of the illuminant in the scene, rendering the acquired objects as if they were lit by an ideal illuminant. The dedicated module is usually referred to as automatic white balance (AWB), which should be able to determine from the image content the color temperature of the ambient light and compensate for its effects. Numerous methods exist in the literature, and Hordley [2] gives an excellent review of them. Once the color of the ambient light has been estimated, the compensation for its effects is generally based on an independent regulation of the three color signals through three different gain coefficients [7]. This correction can be easily implemented on digital devices as a diagonal matrix multiplication.

The second stage of the color correction pipeline is the device chromatic response characterization, which transforms the image data into a standard RGB color space (e.g., sRGB, ITU-R BT.709). This transformation, usually called color matrixing, is needed because the spectral sensitivity functions of the sensor color channels rarely match those of the desired output color space. Typically, this transformation is a 3-by-3 matrix with nine variables to be optimally determined, and both algebraic [3] and optimization-based methods [4] exist to find it.

The typical color correction pipeline can be thus described as follows:

$$\begin{bmatrix} R \\ G \\ B \end{bmatrix}_{\text{out}} = \left( \alpha \begin{bmatrix} a_{11} & a_{12} & a_{13} \\ a_{21} & a_{22} & a_{23} \\ a_{31} & a_{32} & a_{33} \end{bmatrix} \begin{bmatrix} r_{awb} & 0 & 0 \\ 0 & g_{awb} & 0 \\ 0 & 0 & b_{awb} \end{bmatrix} \begin{bmatrix} R \\ G \\ B \end{bmatrix}_{\text{in}} \right), \quad (2)$$

where **RGB**<sub>in</sub> are the camera raw **RGB** values,  $\alpha$  is an exposure compensation common gain, the diagonal matrix  $\text{diag}(r_{awb}, g_{awb}, b_{awb})$  is the channel-independent gain compensation of the illuminant, the full 3-by-3 matrix  $a_{(i,j)}$ ,  $(i,j) = \{1, 2, 3\}^2$  is the color space conversion transform from the device-dependent RGB to the sRGB color space,  $\gamma$  is the gamma correction defined for the sRGB color space (where, for abuse of notation, it is intended to be applied componentwise), and **RGB**<sub>out</sub> are the output sRGB values.

Usually the color matrix transform is optimized for a single illuminant and is applied as it is for all the illuminants that can occur. This could lead to high colorimetric accuracy if the occurring illuminant is the one for which the matrix has been derived (assuming that it is correctly compensated by the AWB module), and low colorimetric accuracy for different illuminants. The first part of the proposed strategy shows how to compute a combined matrix for different classes of commonly occurring illuminants. If only *a priori* probability distribution about the illuminant occurrences is known, the best color matrix can be found offline and applied as it is for all the

shots; if the AWB is able to give a probability distribution about the illuminant in the scene (as color-by-correlation [8] does), an adaptive optimal matrix transform could be found for each shot.

Starting from the observation that the illuminant estimation is not error free and, being an ill-posed problem [9], a perfect algorithm does not exist, the second part of the proposed strategy shows how to derive color correction matrices that, in addition to color space conversion, incorporate information about the illuminant estimation process in order to compensate for its possible errors.

### 3. ILLUMINANT VARYING COLOR CORRECTION MATRIX

In the following, a more compact version of Eq. (2) is used:

$$\mathbf{RGB}_{\text{out}} = (\alpha \mathbf{AD} \cdot \mathbf{RGB}_{\text{in}})^\gamma, \quad (3)$$

where  $\alpha$ , **D**, and **A**, respectively, represent the exposure compensation gain, the diagonal matrix for the illuminant compensation, and the color matrix transformation.

Given a set of  $n$  different patches whose sRGB values **r** are known, and the corresponding camera raw values **c** measured by the sensor when the patches are lit by the chosen illuminant, what is usually done is to find the matrix **M** that satisfies

$$\mathbf{M} = \arg \left( \min_{\mathbf{A} \in \mathbb{R}^{3 \times 3}} \sum_{k=1}^n \mathcal{E}(\mathbf{r}_k, (\alpha \mathbf{AD} \mathbf{c}_k)^\gamma) \right), \quad (4)$$

where  $\mathcal{E}$  is the chosen error metric, and the subscript  $k$  indicates the triplet in the  $k$ th column of the matrix. In this work, the error metric  $\mathcal{E}$  consists of the computation of the average  $\Delta E_{94}$  colorimetric error between the reference and calculated sRGB values mapped in the CIELAB color space. Details about the sRGB to CIELAB conversion and  $\Delta E_{94}$  colorimetric error computation are given in Appendix A. The values of  $\alpha$  and **D** are previously computed in order to perfectly expose the scene and compensate for the illuminant. Given the importance of neutral tones in the color reproduction, usually the 9 degrees of freedom of the color matrix transformation are reduced to 6 by a white point preserving constraint, i.e., a neutral color in the device-dependent color space should be mapped to a neutral color in the device independent color space. This can be easily obtained by constraining each row to sum to 1.

In order to be able to optimize the color matrix transformation under multiple illuminants we have to extend Eq. (4). Let us suppose to consider  $m$  different illuminants, and to have an *a priori* probability distribution  $\mathbf{w} = \{w_1, \dots, w_m\}$  about them. Equation (4) can then be easily extended as

$$\mathbf{M} = \arg \left( \min_{\mathbf{A} \in \mathbb{R}^{3 \times 3}} \sum_{j=1}^m w_j \left( \sum_{k=1}^n \mathcal{E}(\mathbf{r}_k, (\alpha_j \mathbf{AD}_j \mathbf{c}_k)^\gamma) \right) \right) \\ \text{subject to } \sum_{j=1}^3 A_{(i,j)} = 1, \quad \forall i \in \{1, 2, 3\}. \quad (5)$$

Obviously, the probability distribution  $\mathbf{w}$  can also represent the relative importance that we want to give to the errors under each considered illuminant. As for the single illuminant case, the color matrix can be calculated offline and then applied as it is to each different shot.

If we use an AWB algorithm that is able to give information about the probability of the illuminant in the scene, we can use this information to give the best color matrix transform for that illuminant probability distribution. In this case, an adaptive color matrix is applied for each shot, thus leading to more computational requirements. Different strategies can be adopted, ranging from higher to lower computational and memory requirements:

- for each shot, a new optimization could be carried out by using into Eq. (5) the illuminant probability distribution as it comes out from the AWB process;
- all the possible illuminant probability distributions that the AWB could produce in real situations could be quantized and, for each of them, a different optimization could be carried out; the transforms obtained could be stored into a lookup table (LUT). Then for each shot the best color matrix transform could be found by interpolation of the LUT distributions;
- a different optimization could be carried out for each illuminant by using Eq. (4) and storing the color matrix transforms obtained. Hence, the best color matrix transform for each shot could be obtained through a linear combination of the stored transforms by using the illuminant probability distribution provided by the AWB estimation as weighting vector.

#### 4. COLOR CORRECTION MATRIX ROBUST TO ILLUMINANT ESTIMATION ERRORS

In order to give a faithful representation of the scene in the sRGB color space, all the existing color matrix transformations rely on the assumption that the illuminant has been correctly estimated and compensated by the AWB. As mentioned above, the illuminant estimation is an ill-posed problem and the AWB estimation module often fails. The authors also demonstrated that the best AWB algorithm of all does not exist and, for each different algorithm, there are images on which it produces poor results [10]. Moreover, when the AWB fails, the errors in the illuminant estimation and compensation could be even amplified by the color matrix transformation. Inspired by this consideration, we have developed a strategy to compute color matrix transformations assuming an illuminant white point estimation error, i.e., color matrix transformations more robust to illuminant estimation and compensation errors.

Let us consider the case of a single illuminant optimization. The generalization to the multiple illuminant case is straightforward. Suppose that the best gain coefficients  $\mathbf{g}_0 = [r_0, g_0, b_0]$  have already been determined and reshaped in the diagonal transform  $G_0$  to compensate the considered illuminant. The gain coefficients  $\mathbf{g}_0$  can be easily determined taking the inverse of the camera raw values measured by the sensor when a gray patch is acquired under the considered illuminant. To simulate the errors that may occur in the AWB, we can generate a set  $\mathbf{g} = \{g_1, \dots, g_s\}$  of  $s$  gain coefficients with different distances from  $\mathbf{g}_0$ ; in practice, this is done

by sampling the illuminant estimation error space. Different sampling strategies could be used to generate the set  $\mathbf{g}$ ; the one adopted in this work is described in Subsection 6.C. Knowledge about the error distribution in the illuminant estimation can be modeled with a weight distribution  $\mathbf{u} = \{u_0, \dots, u_s\}$  over the set  $\mathbf{g}$ . The weight distribution  $\mathbf{u}$  can be then modified to incorporate the error acceptability in the illuminant estimation for different hue and chroma values. In fact, it has been shown that humans are not equally sensitive to illuminant estimation errors for all the hue and chroma values [11]. The knowledge modeled with the weight distribution  $\mathbf{u}$  can be then exploited during the optimization of the color correction matrix. The optimization problem can be thus formulated as

$$\mathbf{M} = \arg \left( \min_{\mathbf{A} \in \mathbb{R}^{3 \times 3}} \sum_{j=0}^s \mathbf{u}_j \left( \sum_{k=1}^n \mathcal{E}(\mathbf{r}_k, (\alpha_j \mathbf{A} \mathbf{G}_j \mathbf{c}_k)^\gamma) \right) \right)$$

$$\text{subject to } \sum_{j=1}^3 A_{(i,j)} = 1, \quad \forall i \in \{1, 2, 3\}, \quad (6)$$

where  $\mathbf{G}_j$ ,  $j = \{0, \dots, s\}$  are the diagonal matrices obtained, respectively, by reshaping the gain coefficients  $\{g_0, \dots, g_s\}$ . Although very similar to Eq. (5), the idea behind Eq. (6) is quite different.

## 5. EXPERIMENTAL SETUP

All the experiments were performed by using the ISET Digital Camera Simulator [12] developed at Stanford University. This system makes it possible to simulate the entire image processing pipeline of a digital camera, combining both optical modeling and sensor technology simulation. Moreover, the ISET is able to emulate different kinds of noise sources involved in the image acquisition process. As reference camera inside the ISET, we used the widely diffused Nikon DSLR D70, whose sensor spectral sensitivities are known.

## 6. RESULTS AND DISCUSSION

### A. Fixed Color Correction Matrix Optimized for a Single Illuminant, under Ideal Illuminant Estimation Conditions

For the single illuminant case, two different benchmarking algorithms in the state of the art have been used for comparison: the White Point Preserving Least Squares (WPPLS) [3] and an optimization-based algorithm [White Point Preserving Pattern Search (WPPPS)] proposed by the authors [4]. The WPPLS finds the linear transform  $\mathbf{M}$  in Eq. (4) such that the residual squared error is minimized (i.e.,  $\mathcal{E}$  is the  $\mathcal{L}_2$ -norm) under a neutral axis preserving constraint. Given the formulation in the least squares sense, the WPPLS is able to find a closed form solution. The second method, the WPPPS, finds the linear transform in Eq. (4), permitting more general formulations for the error metric  $\mathcal{E}$ . In this paper, we use the average  $\mathcal{L}_1$ -norm, together with its minimum, maximum, and standard deviation under a neutral axis preserving constraint [4]. Given the nature of the error metric considered, a closed form solution does not exist and a direct search method for nonlinear optimization is adopted [4].

The results obtained by the WPPLS and WPPPS are compared with the single illuminant strategy (SILL) described in Eq. (4), where the error metric  $\mathcal{E}$  is the  $\Delta E_{94}$  under a neutral axis preserving constraint. For this comparison, 14 different training illuminants have been considered: six CIE daylight illuminants (D48, D55, D65, D75, D100, D200), three CIE standard illuminants (A, B, C), a 2000 K Planckian blackbody radiator, a uniform white (UW), and three fluorescent illuminants (F2, F7, F11). These are the same used by Finlayson [13] with the addition of the three fluorescent illuminants. The training scenes consisted of the Macbeth ColorChecker (MCC) chart illuminated by each of the training illuminants. The data used for the computation of the color correction matrices were derived directly from the ISET sensor raw data by extracting, for each different patch of the MCC, the mean value of the central area.

In Table 1, the average  $\Delta E_{94}$  colorimetric error obtained by the considered approaches on the training scenes are reported. Fourteen different color matrix transformations were derived (one for each illuminant) and the results under the optimized illuminant are reported. For more details about error statistics see Table 8 in Appendix B.

In Fig. 1, a radar plot is reported to graphically compare the performance obtained by the single illuminant SILL approach under all the 14 training illuminants considered. For better reading, only four different transformations are compared: they are the ones derived for the D65, A, 2000 K, and F11 illuminants; the complete results are reported in Table 9 of Appendix B. It can be noticed that, for each illuminant, the lowest  $\Delta E_{94}$  error is reached by the transformation optimized for that specific illuminant. In particular, the overall best results are obtained for illuminants with a correlated color temperature (CCT) in the range 4800–6500 K, which could suggest a color filter design aimed to optimize the camera color response under average daylight illuminant. These results suggest that relying on a single transformation optimized for a single illuminant is not the best strategy for the color correction module.

**Table 1. Average  $\Delta E_{94}$  Colorimetric Error Obtained by the Color Correction Matrices Optimized for the Different Illuminants, Evaluated on the Same Illuminant for Which the Optimization Is Carried Out**

Illuminant	Method		
	WPPLS	WPPPS	SILL
D48	1.5814	0.8585	0.8213
D55	1.8060	0.7420	0.7175
D65	1.2924	0.7847	0.6454
D75	1.4321	0.7743	0.6333
D100	2.2523	0.7710	0.6871
D200	2.3075	0.9529	0.8745
A	2.9431	1.8278	1.7083
B	2.2336	0.8640	0.8337
C	1.5291	0.6704	0.6289
2000 K	4.7032	3.1238	2.9595
UW	1.3010	1.7990	0.7028
F2	2.2654	1.4226	1.3488
F7	1.4263	3.3418	0.5683
F11	2.6258	1.4277	1.308

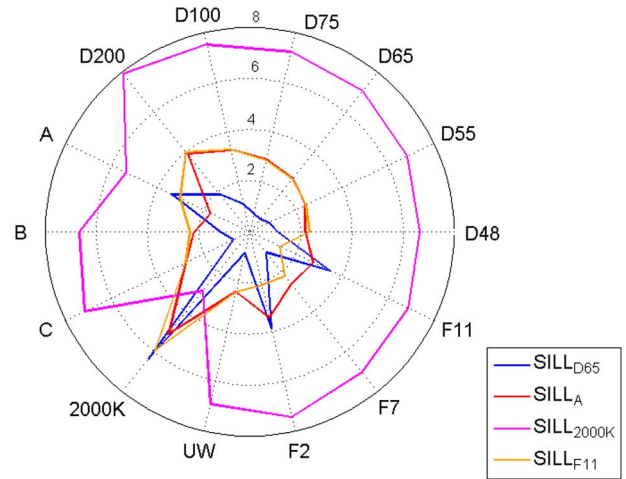


**Fig. 1.** (Color online) Radar plot of the mean  $\Delta E_{94}$  errors obtained under the different illuminants considered by four different SILL approaches optimized for four different illuminants; D65, A, 2000 K, and F11.

## B. Fixed Color Correction Matrix Optimized for Multiple Illuminants, under Ideal Illuminant Estimation Conditions

An alternative approach could be based on the computation of a color matrix transformation optimized simultaneously for multiple illuminants, taking eventually into account an *a priori* probability distribution of the training illuminants. For greater generality, a uniform *a priori* distribution for the illuminant probability in Eq. (5) is adopted here, i.e.,  $\mathbf{w} = \{w_{D48}, w_{D55}, \dots, w_{F7}, w_{F11}\} = \{1/14, \dots, 1/14\}$ . The results obtained on the training scenes are reported in Table 2, where the most expensive and the cheapest strategy exposed in Section 3 are compared. The first one (HILL) is the result of the minimization using Eq. (5) with the uniform *a priori* distribution, the second one (HILLA) is a linear approximation of it: it is the result of the linear combination of the results obtained on the 14 different illuminants considered. It is possible to notice that the two strategies convey almost identical results,

**Table 2. Average  $\Delta E_{94}$  Colorimetric Error Obtained by the Color Correction Matrices Optimized Simultaneously for the Different Illuminants, Evaluated on All the Considered Illuminants**

Illuminant	SILL <sub>D55</sub>	SILL <sub>UW</sub>	HILL	HILLA
D48	0.9093	0.9462	0.9325	0.9326
D55	0.7175	0.7574	0.7495	0.7495
D65	0.7952	0.7910	0.7972	0.7971
D75	0.9852	0.9793	0.9886	0.9870
D100	1.4092	1.4049	1.4220	1.4237
D200	2.1496	2.1320	2.1704	2.1699
A	3.1261	3.1356	3.1444	3.1445
B	0.9454	0.9419	0.9507	0.9510
C	0.9482	0.9010	0.9433	0.9442
2000 K	6.1841	6.1806	6.1903	6.1908
UW	0.7674	0.7028	0.7237	0.7239
F2	3.6511	3.6831	3.5429	3.5415
F7	0.9251	0.9644	0.8432	0.8442
F11	3.1802	3.1513	3.0754	3.0770
avg	1.9067	1.9051	1.8910	1.8912

making it possible to use the cheapest strategy without affecting the color accuracy. A further analysis shows how both the HILL and HILLA strategies, at least on the simulation carried out in these experiments, lead to almost identical results to those obtained by the best SILL approaches (i.e., SILL<sub>D65</sub> and SILL<sub>UW</sub>).

The analysis of Fig. 1 and Table 2 shows that there is not enough room for improvement for the HILL and HILLA strategies. In fact, it is possible to notice that, for example, the SILL<sub>D65</sub> color transform conveys small colorimetric errors for illuminant with a CCT close to the one for which the transformation has been optimized (i.e., 6500 K) and high errors for very distant CCTs. On the other hand, the transformations optimized for very low CCTs (for example, the SILL<sub>2000 K</sub> with a CCT of 2000 K) convey high colorimetric errors for a large number of illuminants. This means that, if we want to lower the colorimetric errors for very low CCTs, we have to decrease the color accuracy for less extreme CCTs. This, at least on the simulation carried out in these experiments with the illuminant probability adopted, does not lead to a significant improvement.

### C. Illuminant Varying Color Correction Matrices under Ideal Illuminant Estimation Conditions

The behavior of the different color transformation matrices under the different illuminants suggests that a greater improvement in color accuracy for all the illuminants could be reached, if we were able to identify the actual illuminant and choose the best color correction matrix for it. In order to test this hypothesis, 1000 different test scenes have been generated. Each of them was composed of a random power of 2 different patches ( $2^k, k \in \mathbb{N}, k \leq 11$ ) extracted from the International Organization for Standardization (ISO) reflectance database [14] and illuminated by a random illuminant extracted from the illuminant test dataset [15]. Three different approaches are tested: the first one is the multiple illuminant ideal case (MILL), i.e., for each of the test illuminants, the best color correction matrix is computed and applied. This is an ideal case, since we assume that we have a color correction matrix optimized for each testing illuminant, and is used to compute the lower bound of the colorimetric error achievable with strategies based on illuminant varying color correction matrices. In the second one (MILLA), the illuminant CCT is first computed and the color correction matrix optimized for the training illuminant with the closest CCT is applied. In the last case (MILLA<sub>2</sub>), the illuminant CCT is first computed, the two training illuminants  $ILL_i$  and  $ILL_j$  with the closest CCTs are identified, and the color correction matrix is calculated as follows:

$$M = \alpha SILL_i + (1 - \alpha) SILL_j, \quad (7)$$

where

$$\alpha = \frac{d(\text{CCT}, \text{CCT}_j)}{d(\text{CCT}, \text{CCT}_i) + d(\text{CCT}, \text{CCT}_j)}.$$

The mean colorimetric error obtained on the test images by the proposed strategies are reported in Table 3. The percentage accuracy improvement with respect to the SILL<sub>D65</sub> is also

**Table 3. Average  $\Delta E_{94}$  Colorimetric Error and Percentage Colorimetric Accuracy Improvement with Respect to the Most Performing Strategy, Obtained by All the Proposed Strategies**

Method	Opt. Illuminant	Mean $\Delta E_{94}$	Improvement
SILL	D48	3.0386	7.31%
SILL	D55	3.1250	4.67%
SILL	D65	3.2782	*
SILL	D75	3.4274	-4.55%
SILL	D100	3.7436	-14.20%
SILL	D200	4.3225	-31.86%
SILL	A	3.3380	-1.82%
SILL	B	3.0628	6.57%
SILL	C	3.3945	-3.55%
SILL	2000 K	7.9029	-141.07%
SILL	UW	3.1422	4.15%
SILL	F2	3.1371	4.30%
SILL	F7	3.0307	7.55%
SILL	F11	2.9857	8.92%
SILL avg	*	3.6378	-9.89%
HILL	$\mathbf{w} = \{1/14, \dots, 1/14\}$	2.9524	9.94%
HILLA	$\mathbf{w} = \{1/14, \dots, 1/14\}$	2.9578	9.77%
MILL	*	2.2002	32.88%
MILLA	*	2.7711	15.47%
MILLA <sub>2</sub>	*	2.6318	19.72%

reported. This is chosen as a benchmarking strategy since a fixed, single color correction matrix optimized for the D65 illuminant is what is usually used for the colorimetric characterization of imaging devices that use sRGB as the output color space.

### D. Color Correction Matrices under Nonideal Illuminant Estimation Conditions

All the experiments made in the previous subsections rely on the assumption that the scene illuminant has been correctly estimated and compensated for. This hypothesis does not often hold. It is known, in fact, that the different white-balance algorithms make errors in the illuminant estimation. Let us examine how the color correction matrix propagates the illuminant estimation error. Let us consider, for example, what happens under the D65 illuminant. To this end, starting from the optimal D65 compensation gains, a set of gains with varying illuminant estimation accuracy levels is generated. The error measure chosen to generate them is the perceptual Euclidean distance (PED) recently proposed by Gijsenij *et al.* [11], but a different choice could be made. The PED consists in a weighted Euclidean distance between the normalized RGB measurements of two illuminants; this measure has been used here since it has been shown to have good correlation with human observers [11]. The gains are generated at 10 different PED magnitudes in 64 different directions in the YCbCr color space, i.e., fixed in a direction in the CbCr plane; the gain along that direction with the desired PED error is found. In Fig. 2(a), a cylindrical plot is reported where, to each combination  $(\rho, \theta)$  representing the magnitude and direction of the PED error, an altitude information is associated, representing the average  $\Delta E_{94}$  error produced on the MCC acquired under the D65 illuminant, corrected with the distorted illuminant gains. In Fig. 2(b), the same plot is represented after the color correction with the SILL<sub>D65</sub> matrix. It is possible to notice that

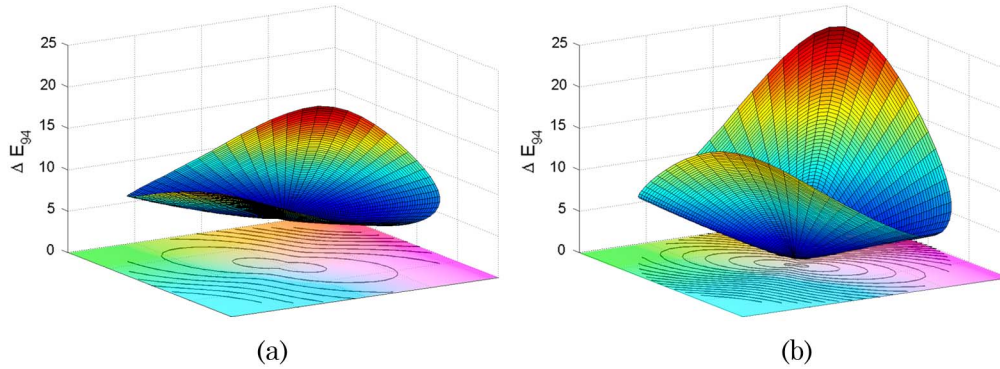


Fig. 2. (Color online)  $\Delta E_{94}$  error distribution as the error in the illuminant estimation and compensation changes under the D65 illuminant: (a) no color correction and (b) SILL<sub>D65</sub> color correction.

the SILL color correction matrix greatly reduces the  $\Delta E_{94}$  when the illuminant has been estimated and corrected with a high accuracy (central part of the plots). The errors become larger as the illuminant estimation precision lowers. The average slopes of the surfaces plotted, 0.6589 for the left one and 1.7306 for the right one, reflect the higher dependency on the illuminant estimation precision of the color correction matrix SILL<sub>D65</sub>. The average slope can also be seen as a measure of the error amplification due to the color correction matrix used: the higher the average slope value, the higher is the error amplification of the illuminant estimation error caused by the color correction matrix used.

The next experiment aims to find color correction matrices less dependent on the precision of the illuminant estimation. This means that, in addition to color space conversion, the color correction matrices will be able to compensate for AWB errors, featuring what we call the white-balance error buffer (WEB). To obtain such matrices, for each of the training illuminants, 1000 different scenes composed of a random power of 2 different patches ( $2^k$ ,  $k \in \mathbb{N}$ ,  $k \leq 11$ ) extracted from the ISO reflectance database are created. In order to estimate such color correction matrices, we have to know or at least suppose, the trends of the AWB illuminant estimation errors [i.e., the weight distribution  $\mathbf{u}$  in Eq. (6)]. Instead of using a general uniform probability, we have preferred to use the error probability distributions of three illuminant estimation algorithms. We have selected the gray world (GW), the white point (WP), and the gamut mapping (GM) algorithms, but a different choice could be made. The GW assumes that the average reflectance in a scene is achromatic, and thus estimates the illuminant color as the average of the colors in the scene [16]. The WP, also known as maximum RGB, assumes that the maximum reflectance in a scene is achromatic and thus estimates the illuminant color as the maximum of the colors in the scene for each channel independently [17]. The GM assumes that, for a given illuminant, one observes only a limited number of colors [18]. It has a training phase in which a canonical illuminant is chosen and the canonical gamut is computed, observing as many surfaces under the canonical illuminant as possible. Given an input image with an unknown illuminant, its gamut is computed and the illuminant is estimated as the mapping that can be applied to the gamut of the input image, resulting in a gamut that lies completely within the canonical gamut and produces the most colorful scene.

Each of the new color correction matrices found, optimized for a SILL-WEB, is compared with the previous one (SILL) op-

timized for the same illuminant on 1000 randomly generated test scenes. Each of them was composed of a random power of 2 different patches ( $2^k$ ,  $k \in \mathbb{N}$ ,  $k \leq 11$ ) extracted from the ISO reflectance database and illuminated by the same training illuminant for which the matrices have been optimized. The results of the comparisons are reported in Table 4. It is possible to notice that both the average  $\Delta E_{94}$  errors and the average slope of the SILL-WEB matrices are lower than the those obtained by the SILL ones. In particular, the lower slope values reflect the minor dependence on the illuminant estimation precision, as well as the lower amplification of the eventual illuminant estimation error. The lower  $\Delta E_{94}$  errors reflect, instead, the fact that the new color correction matrices have learned and are able to compensate to some extent the way the illuminant estimation algorithms fails.

In Table 3, we found that an improvement in color accuracy for all the illuminants could be reached if we were able to identify the actual illuminant and choose the best color correction matrix for it (i.e., the strategies named MILL, MILLA, and MILLA<sub>2</sub>). We want to compare here the MILL, MILLA, and MILLA<sub>2</sub> strategies based on the SILL color correction matrices, against the MILL-WEB, MILLA-WEB, and MILLA<sub>2</sub>-WEB counterparts based on the SILL-WEB color correction matrices. To this end, 1000 different test scenes have been generated. Each of them was composed of a random power

**Table 4. Average  $\Delta E_{94}$  Colorimetric Error and Average Slope of the SILL and SILL-WEB Color Correction Matrices**

Opt. Illuminant	SILL		SILL-WEB	
	Mean $\Delta E_{94}$	Mean Slope	Mean $\Delta E_{94}$	Mean Slope
D48	3.5666	1.5056	3.3481	1.3469
D55	3.5170	1.6056	3.3043	1.4844
D65	3.4892	1.7306	3.2642	1.5893
D75	3.4653	1.8283	3.2220	1.7118
D100	3.4615	1.9940	3.2277	1.8201
D200	3.5125	2.2206	3.2706	2.0165
A	4.3060	1.4236	4.0250	1.3379
B	3.6232	1.4563	3.4134	1.2810
C	3.4786	1.7486	3.2524	1.6258
2000 K	5.4033	2.3989	5.2324	2.1032
UW	3.5039	1.5232	3.2892	1.3853
F2	3.8222	1.3453	3.6657	1.2536
F7	3.4308	1.6958	3.2157	1.6033
F11	3.9514	1.1698	3.7766	1.0743

Table 5. Brief Description of the Color Correction Strategies Compared

Strategy Acronym and Short Description	Number and Type of Color Correction Matrices Used	Incorporating AWB Knowledge?	Color Correction Matrix Selection/Combining Scheme	Additional Info
<b>WPPLS:</b> White Point Preserving Least Squares	One, optimized for a single train illuminant	No	—	Benchmarking strategy proposed in [3]
<b>WPPPS:</b> White Point Preserving Pattern Search	One, optimized for a single train illuminant	No	—	Benchmarking strategy proposed in [4]
<b>SILL:</b> Single ILLuminant	One, optimized for a single train illuminant	No	—	The (optional) subscript indicates the optimizing illuminant
<b>HILL:</b> Hybrid ILLuminant	One, optimized for all train illuminants simultaneously	No	—	The color correction matrix is found using a uniform a-priori distribution for the illuminant probability $w$ in Eq. (5)
<b>HILLA:</b> Hybrid ILLuminant, Approximated	One, optimized for all train illuminants simultaneously	No	Linear combination with uniform weights of the SILL color correction matrices individually optimized for each train illuminant	—
<b>MILL:</b> Multiple ILLuminant	One for each test illuminant	No	—	Ideal case: used for the computation of lower bound performances for MILL* class strategies
<b>MILLA:</b> Multiple ILLuminant, Approximated	One for each train illuminant (14)	No	Selection of the color correction matrix optimized for the train illuminant with the closest CCT to the one in the scene	—
<b>MILLA<sub>2</sub>:</b> Multiple ILLuminant, Approximated with 2 nearest neighbors	One for each train illuminant (14)	No	Linear combination of the two color correction matrices optimized for the train illuminants with the closest CCTs to the one in the scene	—
<b>SILL-WEB:</b> Single ILLuminant with White-balance Error Buffer	One, optimized for a single train illuminant	Yes	—	The (optional) subscript indicates the optimizing illuminant
<b>MILL-WEB:</b> Multiple ILLuminant with White-balance Error Buffer	One for each test illuminant	Yes	—	Ideal case: used for the computation of lower bound performances for MILL*-WEB class strategies
<b>MILLA-WEB:</b> Multiple ILLuminant with White-balance Error Buffer, Approximated	One for each train illuminant (14)	Yes	Selection of the color correction matrix optimized for the train illuminant with the closest CCT to the one in the scene	—
<b>MILLA<sub>2</sub>-WEB:</b> Multiple ILLuminant with White-balance Error Buffer, Approximated with 2 nearest neighbors	One for each train illuminant (14)	Yes	Linear combination of the two color correction matrices optimized for the train illuminants with the closest CCTs to the one in the scene	—

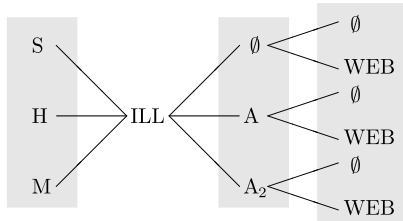


Fig. 3. Composition rules for the generation of the acronyms of the proposed strategies.

of 2 different patches ( $2^k, k \in \mathbb{N}, k \leq 11$ ) extracted from the ISO reflectance database and illuminated by a random illuminant extracted from the illuminant test dataset. Three new different approaches are tested: the first one is the ideal case (MILL-WEB), i.e., for each scene of the test set, the illuminant is estimated and compensated for by using one of the illuminant estimation algorithms considered (i.e., GW, WP, or GM), and then the best color correction matrix is computed and applied. In the second one (MILLA-WEB), the illuminant is first estimated and compensated for by using one of the illuminant estimation algorithms considered, and then the color correction matrix optimized for the training illuminant with the closest gains (estimated with the selected illuminant estimation algorithm) is applied. In the last case (MILLA<sub>2</sub>-WEB), the illuminant compensation gains are first computed with one of the illuminant estimation algorithms considered, then the two training illuminants  $ILL_i$  and  $ILL_j$  with the closest gains are identified and the color correction matrix is calculated as follows:

$$M = \alpha \text{SILL-WEB}_i + (1 - \alpha) \text{SILL-WEB}_j, \quad (8)$$

where

$$\alpha = \frac{\text{PED}(\text{gains}, \text{gains}_j)}{\text{PED}(\text{gains}, \text{gains}_i) + \text{PED}(\text{gains}, \text{gains}_j)}. \quad (9)$$

In Table 5, a brief description of the main features of the color correction strategies compared is reported: the strategies are grouped into classes on the basis of the type and number of color correction matrices that they use. All the strategies compared use the same type of matrices for the illuminant compensation, i.e., diagonal matrices. All the color

correction matrices used are optimized under a neutral axis preserving constraint.

The acronyms of the proposed strategies are generated using the scheme reported in Fig. 3.

The first part indicates the number and type of the color correction matrix used (SILL = Single ILLuminant, a single matrix optimized for a fixed single illuminant; HILL = Hybrid ILLuminant, a single matrix optimized for multiple illuminants simultaneously; MILL = Multiple ILLuminant, multiple matrices each optimized for a different single illuminant). The second part indicates if and what kind of approximation has been used ( $\emptyset$  = not approximated, A = Approximated, and A<sub>2</sub> = Approximated with two nearest neighbors). The third part indicates if the strategy implements color correction matrices able to compensate for AWB errors (WEB = White-balance Error Buffer) or not ( $\emptyset$ ). The symbol  $\emptyset$  is reported in the scheme but is intended as the null character and thus omitted in the acronyms generated.

The mean colorimetric errors obtained on the test images by all the proposed strategies are reported in Table 6. From the analysis of Table 6, it is possible to notice that the lowest colorimetric errors are achieved using the approaches based on the use of color correction matrices optimized incorporating knowledge about the AWB module behavior (i.e., approaches with the suffix WEB, described in Section 4). To understand if the differences among the different color correction strategies considered are statistically significant, and what their ranking is, we have used the Wilcoxon signed-rank test [19]. This statistical test permits us to compare the whole error distributions without limiting to punctual statistics. Furthermore, it is well suited because it does not make any assumptions about the underlying error distributions, and it is easy to find by using, for example, the Lilliefors test [20], that the assumption about the normality of the error distributions does not always hold. Let  $X$  and  $Y$  be random variables representing the  $\Delta E_{94}$  colorimetric errors obtained on all the patches of the 1000 test scenes by the color correction strategies  $M_X$  and  $M_Y$ ; let  $\mu_X$  and  $\mu_Y$  be the median values of such random variables. The Wilcoxon signed-rank test can be used to test the null hypothesis  $H_0: \mu_X = \mu_Y$  against the alternative hypothesis  $H_1: \mu_X \neq \mu_Y$ . We can test  $H_0$  against  $H_1$  at a given significance level  $\alpha$ . We reject  $H_0$  and accept  $H_1$  if the probability of observing the error differences we obtained is less than or equal to  $\alpha$ . We have used the alternative

**Table 6. Average  $\Delta E_{94}$  Colorimetric Error and Percentage Colorimetric Accuracy Improvement with Respect to the State-of-the-Art Strategy (SILL<sub>D65</sub>), Obtained by All the Proposed Strategies**

Method	Illuminant Estimation Algorithm Used					
	Gray World (GW)		White Point (WP)		Gamut Mapping (GM)	
	Mean $\Delta E_{94}$	Improvement	Mean $\Delta E_{94}$	Improvement	Mean $\Delta E_{94}$	Improvement
SILL <sub>D65</sub>	5.2252	*	4.8796	*	3.4939	*
MILL	4.5907	12.14%	3.9803	18.43%	2.9947	16.67%
MILLA	4.9384	5.49%	4.3974	10.97%	3.2210	8.47%
MILLA <sub>2</sub>	4.7171	9.72%	4.1643	17.18%	3.1119	12.27%
SILL-WEB <sub>D65</sub>	4.7260	9.55%	4.4061	10.75%	3.1469	11.03%
MILL-WEB	3.8805	25.73%	3.1978	52.59%	2.5169	38.82%
MILLA-WEB	4.4420	14.99%	4.1272	18.23%	2.9066	20.21%
MILLA <sub>2</sub> -WEB	4.2214	19.21%	3.8707	26.07%	2.7857	25.42%

hypothesis  $H_1 : \mu_X < \mu_Y$  with a significance level  $\alpha = 0.05$ . The outputs of the statistical test are reported in Table 7. A “+” sign in the  $(i, j)$  position of the table means that the color correction strategy  $i$  has been considered statistically better than the color correction strategy  $j$ ; a “-” sign means that it has been considered statistically worse, and a “=” sign means that they have been considered statistically equivalent. The count of the number of times that a color correction strategy has been considered statistically better than the others gives us a score, which is reported in the last column of the table.

**Table 7. (Color online) Outputs of the Statistical Test for the Color Correction Strategies Considered<sup>a</sup>**

(a)									
	SILL <sub>D65</sub>	MILL	MILLA	MILLA <sub>2</sub>	SILL-WEB <sub>D65</sub>	MILL-WEB	MILLA-WEB	MILLA <sub>2</sub> -WEB	Score
SILL <sub>D65</sub>	=	-	-	-	-	-	-	-	0
MILL	+	=	+	+	+	-	-	-	4
MILLA	+	-	=	-	-	-	-	-	1
MILLA <sub>2</sub>	+	-	+	=	=	-	-	-	2
SILL-WEB <sub>D65</sub>	+	-	+	=	=	-	-	-	2
MILL-WEB	+	+	+	+	+	=	+	+	7
MILLA-WEB	+	+	+	+	+	-	+	-	5
MILLA <sub>2</sub> -WEB	+	+	+	+	+	-	+	=	6

(b)									
	SILL <sub>D65</sub>	MILL	MILLA	MILLA <sub>2</sub>	SILL-WEB <sub>D65</sub>	MILL-WEB	MILLA-WEB	MILLA <sub>2</sub> -WEB	Score
SILL <sub>D65</sub>	=	-	-	-	-	-	-	-	0
MILL	+	=	+	+	+	-	+	-	5
MILLA	+	-	=	-	=	-	-	-	1
MILLA <sub>2</sub>	+	-	+	=	+	-	=	-	3
SILL-WEB <sub>D65</sub>	+	-	=	-	=	-	-	-	1
MILL-WEB	+	+	+	+	+	=	+	+	7
MILLA-WEB	+	-	+	+	+	-	=	-	3
MILLA <sub>2</sub> -WEB	+	+	+	+	+	-	+	=	6

(c)									
	SILL <sub>D65</sub>	MILL	MILLA	MILLA <sub>2</sub>	SILL-WEB <sub>D65</sub>	MILL-WEB	MILLA-WEB	MILLA <sub>2</sub> -WEB	Score
SILL <sub>D65</sub>	=	-	-	-	-	-	-	-	0
MILL	+	=	+	+	+	-	-	-	4
MILLA	+	-	=	-	-	-	-	-	1
MILLA <sub>2</sub>	+	-	+	=	=	-	-	-	2
SILL-WEB <sub>D65</sub>	+	-	+	=	=	-	-	-	2
MILL-WEB	+	+	+	+	+	=	+	+	7
MILLA-WEB	+	+	+	+	+	-	=	-	5
MILLA <sub>2</sub> -WEB	+	+	+	+	+	-	+	=	6

<sup>a</sup>The sign in the  $(i, j)$  position of the table means that the strategy  $i$  is statistically better than the sampling  $j$  (“+” sign), statistically worse (“-” sign), or equivalent (“=” sign). The score is the number of times that a sampling strategy has been considered statistically better than the others. A different table is reported for each of the illuminant estimation algorithms considered: (a) GM, (b) WP, and (c) GM.

From the results of the statistical test reported in Table 7, it is possible to conclude that the strategies based on multiple color correction matrices each optimized for a different illuminant produce significantly lower colorimetric errors with respect to those based on a single color correction matrix (i.e., strategies with MILL prefix are better than the ones with SILL prefix). Being able to accurately estimate the scene illuminant and deriving an optimal color correction matrix for it produces significantly lower colorimetric errors than using a fixed number of precomputed color correction matrices (i.e., MILL is better than MILLA and MILLA<sub>2</sub>). The use of a single color correction matrix optimized incorporating knowledge about AWB module behavior permits us to obtain almost statistically equivalent colorimetric errors with respect to the ones obtained with strategies using a fixed number of precomputed color correction matrices (i.e., SILL-WEB<sub>D65</sub> is almost equivalent to MILLA and MILLA<sub>2</sub>). Finally, the use of strategies based on multiple color correction matrices each optimized for a different illuminant incorporating knowledge about AWB module behavior produce significantly lower colorimetric errors with respect to those based on a single color correction matrix optimized by incorporating knowledge about AWB module behavior (i.e., prefix MILL-WEB strategies are better than prefix SILL-WEB ones).

## 7. CONCLUSIONS

In this paper we have investigated the interactions between the illuminant estimation process and the color correction matrix in the formation of the overall color accuracy, especially when the white point estimation is imperfect. We have shown how the color correction transform amplifies the illuminant estimation errors. Furthermore, we have shown that it is possible to incorporate knowledge about the illuminant estimation behavior in the optimization of the color correction matrix in order to alleviate the error amplification. We have demonstrated that an *a priori* fixed color correction matrix is not able to produce a good color accuracy when the scene illuminant is different from the illuminant adopted for the color correction matrix calculation. We have designed different strategies that are able to improve color accuracy under both perfect and nonperfect illuminant estimation. The experimental results obtained using the ISET digital camera simulator showed that, with respect to a fixed color correction matrix optimized for the D65 illuminant, the proposed strategies make it possible to obtain significant color accuracy improvements. In particular, the best adaptive color transform (i.e., MILLA<sub>2</sub>-WEB) decreased the colorimetric error by 19.72% for the perfect illuminant estimation case (i.e., ideal illuminant estimation). For the nonperfect illuminant estimation case, three different illuminant estimation algorithms have been used: GW, WP, and GM; the best adaptive color transform decreased the colorimetric error by 19.21%, 26.07%, and 25.42%, respectively.

The experimental results also show that, while failures in illuminant estimation have the largest impact on the quality of color reproduction, there are other sources of error that prevent the color reproduction from being perfect. A first source of error is the fact that the sensor RGB spectral sensitivities are not the same as cone spectral sensitivities, nor can they be exactly mapped into each other with a linear transform (i.e., the Luther condition [21] does not hold).

A second source of error is the presence of different kinds of noise that affect sensor measurements. A further source of error is due to the fact that the illuminant correction method adopted is not able to produce a perfect correction for any color, even when the scene illuminant is precisely known. The method used is limited to an adjustment in sensor gain only (i.e., diagonal transforms); as suggested by a reviewer, the use of illuminant-dependent full  $3 \times 3$  corrections should be investigated.

### APPENDIX A: CONVERSION FROM sRGB TO CIELAB AND $\Delta E_{94}$ COLORIMETRIC DIFFERENCE

The conversion from sRGB to CIELAB is done in two steps: from sRGB to CIEXYZ [22], and then from CIEXYZ to CIELAB [23]. The sRGB values are first linearized. We assume that the sRGB values are normalized in the  $[0, 1]$  range. The linearization transform is the same for each channel  $C = \{R, G, B\}$ :

$$C = \begin{cases} C/12.92, & \text{if } C \leq 0.04045 \\ ((C + 0.055)/1.055)^{2.4}, & \text{if } C > 0.04045 \end{cases}$$

The linearized RGB values can be then converted in XYZ through a matrix multiplication:

$$\begin{bmatrix} X \\ Y \\ Z \end{bmatrix} = \begin{bmatrix} 0.4124564 & 0.3575761 & 0.1804375 \\ 0.2126729 & 0.7151522 & 0.0721750 \\ 0.0193339 & 0.1191920 & 0.9503041 \end{bmatrix} \begin{bmatrix} R \\ G \\ B \end{bmatrix}$$

The conversion from CIEXYZ to CIELAB requires a reference white  $[X_r \ Y_r \ Z_r]$ . We have chosen the CIE D65 reference white, with coordinates  $[0.95047 \ 1.0000 \ 1.08883]$ . First, the CIEXYZ coordinates are scaled by the reference white:  $[X \ Y \ Z] = [X/X_r \ Y/Y_r \ Z/Z_r]$ . For each color channel  $C = \{X, Y, Z\}$ :

$$f_C = \begin{cases} C^{1/3}, & \text{if } C > \epsilon \\ (\kappa C + 16)/116, & \text{if } C \leq \epsilon \end{cases}$$

with  $\epsilon = 0.008856$  and  $\kappa = 903.3$ . The CIELAB coordinates are then obtained as

$$\begin{bmatrix} L \\ a \\ b \end{bmatrix} = \begin{bmatrix} 116f_Y - 16 \\ 500(f_X - f_Y) \\ 200(f_Y - f_Z) \end{bmatrix}$$

The colorimetric difference  $\Delta E_{94}$  [24] between a sample color with CIELAB coordinates  $[L_2 \ a_2 \ b_2]$  and a reference color with coordinates  $[L_1 \ a_1 \ b_1]$  is defined as

$$\Delta E_{94} = \sqrt{\left(\frac{\Delta L}{K_L S_L}\right)^2 + \left(\frac{\Delta C}{K_C S_C}\right)^2 + \left(\frac{\Delta H}{K_H S_H}\right)^2}$$

where  $\Delta(\cdot) = (\cdot)_1 - (\cdot)_2$ ,  $\Delta H = \sqrt{\Delta a^2 + \Delta b^2 - \Delta C^2}$ ,  $C = \sqrt{a^2 + b^2}$ ,  $S_L = 1$ ,  $S_C = 1 + K_1 C_1$ ,  $S_H = 1 + K_2 C_1$ ,  $[K_L \ K_C \ K_H] = [1 \ 1 \ 1]$ , and  $[K_1 K_2] = [0.0450.015]$ , which are the values suggested for graphic arts.

### APPENDIX B: ADDITIONAL TABLES

In Table 8, the minimum, mean, maximum, and standard deviation of the  $\Delta E_{94}$  colorimetric error obtained by the considered approaches on the training scenes are reported. The colorimetric errors are valued on scenes generated with the same illuminant for which the specific color correction matrix was optimized.

In Table 9, we report the average  $\Delta E_{94}$  colorimetric errors obtained by the color correction matrices individually optimized for the different illuminants and then evaluated on

**Table 8. Statistics for the  $\Delta E_{94}$  Colorimetric Error Obtained by the Color Correction Matrices Optimized for the Different Illuminants, Evaluated on the Same Illuminant for Which the Optimization Is Carried Out**

Illuminant	Method	Min	Mean	Median	Max	Std
D48	WPPLS	0.4179	1.5814	1.3563	3.9946	1.0080
	WPPPS	0.0230	0.8585	0.6299	4.3109	0.9612
	SILL	0.0114	0.8213	0.5623	4.4062	0.9577
D55	WPPLS	0.4399	1.8060	1.5026	4.9417	1.1727
	WPPPS	0.0692	0.7420	0.5533	3.6860	0.8024
	SILL	0.0257	0.7175	0.5212	3.6407	0.7831
D65	WPPLS	0.4056	1.2924	0.9478	4.0091	0.9552
	WPPPS	0.0171	0.7847	0.6603	3.2856	0.7468
	SILL	0.0533	0.6454	0.4674	3.0602	0.6596
D75	WPPLS	0.4080	1.4321	1.2494	3.9956	0.8514
	WPPPS	0.0641	0.7743	0.5132	2.8967	0.7017
	SILL	0.0760	0.6333	0.4985	2.8013	0.6131
D100	WPPLS	0.7918	2.2523	1.8076	5.1838	1.2901
	WPPPS	0.0093	0.7710	0.5056	2.9846	0.7647
	SILL	0.0780	0.6871	0.6009	2.8135	0.6404
D200	WPPLS	0.8414	2.3075	2.4154	3.3730	0.6708
	WPPPS	0.0217	0.9529	0.6037	3.8108	0.9297
	SILL	0.0390	0.8745	0.6948	3.5975	0.8381
A	WPPLS	0.7814	2.9431	1.9984	9.7471	2.1096
	WPPPS	0.0129	1.8278	1.1124	9.1925	2.1240
	SILL	0.0491	1.7083	0.8344	8.9678	2.1411
B	WPPLS	0.2074	2.2336	1.8791	5.8973	1.7048
	WPPPS	0.0317	0.8640	0.6627	4.1517	0.9303
	SILL	0.0292	0.8337	0.6168	4.3472	0.9624
C	WPPLS	0.4818	1.5291	1.3728	3.0041	0.6567
	WPPPS	0.0396	0.6704	0.4380	3.0910	0.7027
	SILL	0.0279	0.6289	0.4475	2.9747	0.6605
2000 K	WPPLS	1.9435	4.7032	4.2830	8.0833	1.8531
	WPPPS	0.5961	3.1238	1.6654	14.2835	3.2635
	SILL	0.2112	2.9595	1.4862	15.3819	3.6402
UW	WPPLS	0.1984	1.3010	1.2808	2.9917	0.7966
	WPPPS	0.1286	1.7990	1.2915	6.1698	1.5562
	SILL	0.0915	0.7028	0.5855	3.0210	0.6685
F2	WPPLS	0.5355	2.2654	1.7426	4.9969	1.2462
	WPPPS	0.0037	1.4226	0.6329	4.8860	1.4983
	SILL	0.0036	1.3488	0.8667	5.5046	1.4042
F7	WPPLS	0.6094	1.4263	1.4061	2.6802	0.5767
	WPPPS	0.0970	3.3418	3.1368	10.8883	2.9092
	SILL	0.0110	0.5683	0.4116	2.9742	0.6324
F11	WPPLS	0.7488	2.6258	2.3248	8.1779	1.8282
	WPPPS	0.0129	1.4277	0.9201	5.2315	1.4583
	SILL	0.0054	1.3085	0.8711	6.1566	1.4445

**Table 9. Average  $\Delta E_{94}$  Colorimetric Error Obtained by the Color Correction Matrices Optimized Individually for the Different Illuminants, Evaluated on All the Illuminants Considered**

Opt. Illuminant	Viewing Illuminant														Avg.
	D48	D55	D65	D75	D100	D200	A	B	C	2000 K	UW	F2	F7	F11	
D48	0.8213	0.8317	1.0129	1.2220	1.6491	2.3626	2.8787	0.8723	1.1586	6.0337	0.9039	3.5215	1.0178	2.9638	1.9464
D55	0.9093	0.7175	0.7952	0.9852	1.4092	2.1496	3.1261	0.9454	0.9482	6.1841	0.7674	3.6511	0.9251	3.1802	1.9067
D65	1.1327	0.8442	0.6454	0.7357	1.1323	1.8831	3.4034	1.1794	0.7225	6.3473	0.8435	3.9105	1.0456	3.5043	1.9521
D75	1.3468	1.0297	0.7414	0.6333	0.9256	1.6689	3.6139	1.3973	0.6573	6.4685	1.0264	4.1693	1.2333	3.7911	2.0502
D100	1.7653	1.4380	1.0913	0.8645	0.6871	1.2904	3.9945	1.8143	0.9547	6.6999	1.4309	4.7326	1.6906	4.3710	2.3447
D200	2.5161	2.1995	1.8357	1.5540	1.1329	0.8745	4.6530	2.5532	1.6620	7.1161	2.1830	5.6369	2.5495	5.2055	2.9766
A	2.1816	2.4159	2.6934	2.9193	3.3120	3.9167	1.7083	2.1853	2.8036	5.1161	2.4118	3.4623	2.6127	2.7670	2.8933
B	0.8511	0.8259	1.0160	1.2312	1.6613	2.3652	2.9022	0.8337	1.1192	6.0660	0.8528	3.5571	1.0447	2.9772	1.9503
C	1.2740	0.9760	0.7198	0.6609	0.9909	1.7328	3.5564	1.3010	0.6289	6.4578	0.9490	4.1136	1.2004	3.7020	2.0188
2000 K	6.6634	6.8535	7.0755	7.2447	7.5241	7.9369	5.3768	6.6859	7.1736	2.9595	6.9148	7.4405	7.0510	6.8837	6.6989
UW	0.9462	0.7574	0.7910	0.9793	1.4049	2.1320	3.1356	0.9419	0.9010	6.1806	0.7028	3.6831	0.9644	3.1513	1.9051
F2	3.1898	3.2267	3.3946	3.5966	4.0300	4.7823	3.8891	3.2199	3.5582	6.6765	3.2962	1.3488	2.6552	2.1881	3.5037
F7	1.1856	1.0180	1.0394	1.1953	1.6242	2.4070	3.3278	1.2051	1.1908	6.3351	1.0176	3.1048	0.5683	2.9159	2.0096
F11	2.3482	2.4477	2.6733	2.8996	3.3302	4.0055	3.0374	2.3541	2.7909	5.9770	2.4343	2.1346	2.2188	1.3085	2.8543

all the training illuminants considered. The results are reported only for the most performing SILL strategy.

## ACKNOWLEDGMENTS

Our investigation was performed as a part of an ST Microelectronics' research contract. The authors thank the anonymous reviewers for their valuable comments and suggestions for improving the quality of the paper.

## REFERENCES

- R. Ramanath, W. E. Snyder, Y. Yoo, and M. S. Drew, "Color image processing pipeline," *IEEE Signal Process. Mag.* **22**(1), 34–43 (2005).
- S. D. Hordley, "Scene illuminant estimation: past, present, and future," *Color Res. Appl.* **31**, 303–314 (2006).
- P. M. Hubel, J. Holm, G. D. Finlayson, and M. S. Drew, "Matrix calculations for digital photography," *Proceedings of the IS&T/SID Fifth Color Imaging Conference: Color Science, Systems, and Applications* (Society for Imaging Science and Technology, 1997), pp. 105–111.
- S. Bianco, F. Gasparini, A. Russo, and R. Schettini, "A new method for RGB to XYZ transformation based on pattern search optimization," *IEEE Trans. Consum. Electron.* **53**, 1020–1028 (2007).
- P. D. Burns and R. S. Berns, "Error propagation analysis in color measurement and imaging," *Color Res. Appl.* **22**, 280–289 (1997).
- B. E. Bayer, "Color imaging array," U.S. patent 3,971,065 (20 July 1976).
- J. von Kries, "Chromatic adaptation," in *Festschrift der Albrecht-Ludwig-Universität* (Fribourg, 1902). Translation by D. L. MacAdam, *Sources of Color Science* (MIT Press, 1970).
- G. D. Finlayson and S. D. Hordley, "Color by correlation: a simple, unifying framework for color constancy," *IEEE Trans. Pattern Anal. Mach. Intell.* **23**, 1209–1221 (2001).
- Y. Yang and A. Yuille, "Sources from shading," in *IEEE Conference on Computer Vision and Pattern Recognition CVPR '91* (IEEE Computer Society, 1991), pp. 534–539.
- S. Bianco, F. Gasparini, and R. Schettini, "Consensus based framework for illuminant chromaticity estimation," *J. Electron. Imaging* **17**, 023013 (2008).
- A. Gijssenij, T. Gevers, and M. P. Lucassen, "A perceptual analysis of distance measures for color constancy," *J. Opt. Soc. Am. A* **26**, 2243–2256 (2009).
- J. Farrell, F. Xiao, P. Catrysse, and B. Wandell, "A simulation tool for evaluating digital camera image quality," *Proc. SPIE* **5294**, 124–131 (2003).
- G. D. Finlayson, "Color constancy in diagonal chromaticity space," in *IEEE Proceedings of Fifth International Conference on Computer Vision* (IEEE Computer Society, 1995), pp. 218–223.
- "Graphic technology—Standard object colour spectra database for colour reproduction evaluation (SOCS)," Technical Report ISO/TR 16066:2003(E) (International Organization for Standardization, 2003).
- K. Barnard, V. Cardei, and B. Funt, "A comparison of computational color constancy algorithms. I: Methodology and experiments with synthesized data," *IEEE Trans. Image Process.* **11**, 972–984 (2002).
- G. Buchsbaum, "A spatial processor model for object color perception," *J. Franklin Inst.* **310**, 1–26 (1980).
- E. H. Land, "The retinex theory of color vision," *Sci. Am.* **237**(6), 108–128 (1977).
- D. A. Forsyth, "A novel algorithm for color constancy," *Int. J. Comput. Vis.* **5**, 5–35 (1990).
- F. Wilcoxon, "Individual comparisons by ranking methods," *Biometrics* **1**, 80–83 (1945).
- H. Lilliefors, "On the Kolmogorov-Smirnov test for normality with mean and variance unknown," *J. Am. Stat. Assoc.* **62**, 399–402 (1967).
- N. Ohta and A. R. Robertson, *Colorimetry: Fundamentals and Applications* (Wiley, 2005).
- M. Stokes, M. Anderson, S. Chandrasekar, and R. Motta, "A standard default color space for the Internet—sRGB," Version 1.10 (5 Nov. 1996) [www.w3.org/Graphics/Color/sRGB.html](http://www.w3.org/Graphics/Color/sRGB.html).
- G. Wyszecki and W. S. Stiles, *Color Science: Concepts and Methods, Quantitative Data and Formulas* (Wiley, 1967).
- G. Sharma, *Digital Color Imaging Handbook* (CRC Press, 2003).